UNITED STATES PATENT AND TRADEMARK OFFICE

UNITED STATES DEPARTMENT OF COMMERCE
United States Patent and Trademark Office
Address: COMMISSIONER FOR PATENTS
P.O. Box 1450
Alexandria, Virginia 22313-1450
www.uspto.gov

APPLICATION NO.	FILING DATE	FIRST NAMED INVENTOR	ATTORNEY DOCKET NO.	CONFIRMATION NO.
10/582,215	06/08/2006	Robert Greiner	4001-1220	3850

466 7590 01/06/2012

YOUNG & THOMPSON
209 Madison Street
Suite 500
Alexandria, VA 22314

EXAMINER	
KHATRI, PRASHANT J	
ART UNIT	PAPER NUMBER
1783	

NOTIFICATION DATE	DELIVERY MODE
01/06/2012	ELECTRONIC

Please find below and/or attached an Office communication concerning this application or proceeding.

The time period for reply, if any, is set in the attached communication.

Notice of the Office communication was sent electronically on above-indicated "Notification Date" to the following e-mail address(es):

DocketingDept@young-thompson.com

UNITED STATES PATENT AND TRADEMARK OFFICE

BOARD OF PATENT APPEALS AND INTERFERENCES

Ex parte ROBERT GREINER,
HEINRICH KAPITZA and MANFRED OCHSENKUHN

Appeal 2011-006178
Application 10/582,215
Technology Center 1700

Before: FRED E. McKELVEY, RICHARD TORCZON and SALLY GARDNER LANE, *Administrative Patent Judges*.

McKELVEY, *Administrative Patent Judge*.

DECISION ON APPEAL

Statement of the case

Siemens Aktiengesellschaft ("Siemens"), the real party in interest (Brief, page 1), seeks review under 35 U.S.C. § 134(a) of a final rejection dated 19 April 2010.

The application was filed on 8 June 2006. The application on appeal (1) is a § 371 National Stage application of International Application PCT/EP2004/053381, filed 9 December 2004 and (2) claims priority of German application 10358342.4, filed 12 December 2003.

The application has been published as U.S. Patent Application Publication 2007/0158617 A1.

Claims 9, 12, 16-17, 19 and 21-22 are on appeal.

The Examiner relies on the following evidence:

Kosuga et al. "Kosuga"	U.S. Patent 4,960,642	2 Oct. 1990
Matsumoto et al. "Matsumoto"	U.S. Patent Application Publication 2003/0153223 A1	14 Aug. 2003 (filed 24 Dec. 2002)
Nakazawa	Japanese patent application publication 09-241420	16 Sept. 1997

Siemens does not contest the prior art status of the evidence relied upon by the Examiner.

We have jurisdiction under 35 U.S.C. § 134(a).

Findings of fact

The following findings of fact are supported by a preponderance of the evidence.

Additional findings as necessary may appear in the Discussion portion of the opinion.

References to the Specification are to the application as published. The pages of the Specification do not have line or paragraph numbers.

The invention

The Siemens invention relates to a metal/plastic hybrid material which comprises a [1] thermoplastic, [2] a metal compound melting in the range between 100 °C. and 400 °C. and [3] an electrically conducting and/or metallic filler. ¶ 0006.

The object of the Siemens invention is a material, capable of being processed by conventional plastic molding processes (injection molding etc.), and having a high electrical and thermal conductivity. ¶ 0005.

Composition 1.1 is an example of a Siemens invention material. The material is described as including [1] Polyamide 6 (PA 6), [2] a low melting-point metal alloy identified as MCP 200 from HEK GmbH, Lubeck, Germany and having, melting point of 200 °C. and [3] copper fibers having a length of approximately 2 mm and a thickness of approximately 80 µm. Items [1] through [3] are said to be present in the following weight percent ratios:

PA 6 : MCP 200 : Cu fibers = 20 : 20 : 60.

Properties of the material are said to be:

Specific volume resistance: 2.7 x 10^{-3} Ωcm

Specific conductivity: 3.7 x 10^{2} (1 / Ωcm).

See ¶¶ 0024 through 0029.

The Specification does not identify the precise nature of MCP 200. An Internet search on 28 December 2011 reveals that MCP 200 is probably the eutectic of the tin-zinc system. *See*:

http://mcpmetspec.thomasnet.com/item/low-melting-point-alloys/mcp200-metspec-390/item-1012

Siemens describes the melting point as being 200 ºC, whereas the manufacturer describes the melting point as 197 ºC.

Claims on appeal

The claimed invention is narrower than the invention described in the Siemens Specification, as filed.

Claims 9, 16 and 19 are the three independent claims, all having differences in scope.

Claim 9, which we reproduce from the Claims Appendix of the Appeal Brief, reads [matter in brackets added; limitations in issue italicized]:

Claim 9

A metal/plastic hybrid [material] which comprises:

[1] a thermoplastic in a proportion of *10% to 25%* by weight,

[2] a metal compound melting in the range between 100 ºC and 400 ºC[,] the metal compound consisting essentially of a metal

selected from the group consisting of bismuth, zinc, tin and mixtures thereof, and

[3] an electrically conducting and/or metallic filler in the form of a *copper fiber* in a proportion of at least 30% by weight to 70% by weight, and is present jointly with the metal compound melting in the range between 100 °C and 400 °C in the hybrid as a fiber *network*, wherein,

[a] the total proportion of (i) the metal compound melting in the range between 100 °C and 400 °C and (ii) the copper fiber is ≥ 60% by weight, and

[b] *the length of the copper fibers lies between 1 and 10 mm, [and] the thickness is < 100 μm.*

Claim 16

Claim 16, which we reproduce from the Claims Appendix of the Appeal Brief, reads [matter in brackets, indentation added (see 37 C.F.R. § 1.75(i)); limitations in issue italicized]:

A shaped body,

[A] produced by a plastic shaping process, and

[B] which is at least in part manufactured from a metal/plastic hybrid [material] comprising[:]

[1] a thermoplastic in a proportion of *10% to 25%* by weight,

[2] a metal compound melting in the range between 100 °C and 400 °C, the metal compound consisting essentially of a material

selected from the group consisting of bismuth, zinc, tin and mixtures thereof, and

[3] an electrically conducting and/or metallic filler in the form of a *copper fiber* in a proportion of at least 30% by weight to 70% by weight,

wherein the total proportion of (i) the metal compound melting in the range between 100 ºC and 400 ºC and (ii) the copper fiber is ≥ 60% by weight.

Claim 19

Claim 19, which we reproduce from the Claims Appendix of the Appeal Brief, reads [matter in brackets added; limitations in issue italicized]:

A metal/plastic hybrid [material], comprising:

[1] a thermoplastic in a proportion of *10% to 25%* by weight;

[2] a lead-free metal compound melting in the range between 100ºC and 400ºC, the lead-free metal compound consists essentially of a metal; and

[3] an electrically conducting and/or metallic filler in the form of a copper fiber in a proportion between 30% by weight and 70% by weight, wherein,

(a) the *copper fiber* is fused with the lead-free metal compound to provide a fiber *network*, and

(b) the total proportion of (i) the metal compound melting in the range between 100 ºC and 400 ºC and (ii) the copper fiber is ≥ 60% by weight.

Scope and content of the prior art

Matsumoto

The Matsumoto invention generally relates *inter alia* to an electrically conductive plastic material. ¶¶ 0002 and 0010.

Electrically conductive plastic materials that may be used in the Matsumoto invention include a resin formed by combining a matrix resin and an electrically conductive material (filler or filler agent) to form a *net structure* of electrically conductive material in the matrix resin. The matrix resin is not necessarily electrically conductive by itself. When the matrix resin is not conductive, it will be necessary to include a conducting filler in the resin. As a filler, a metal or carbon black may be used. The filler should preferably be capable of being dispersed in the matrix resin and should possess a *net structure* mutually electrically connected within the resin, such as powder or *fiber*. Filler in the form of a powder is quite desirable as it improves the forming performance of the electrically conductive plastic material. Filler in the form of *fibers* may generate anisotropy[1] when the electrically conductive plastic material is formed by injection molding. ¶ 0023.

The preferred filler is a metal. The use of a filler that includes a low

[1] Matsumoto is an English language document probably translated from a document originally in Japanese. In context, we understand "anisotropy" to mean that when injection molding takes place, non-uniformity (and therefore decreased electrical conductivity) of the conducting filler may occur.

melting point metal or a metal alloy is said to be particularly useful. By using a low melting point metal material as a filler, electrical connection is said to be achieved by metallic bond between (1) the filler in the resin and (2) the metal material (*e.g.*, the leads of an LED—discussed in more detail later in this opinion). According to Matsumoto, the metal used as a filler also preferably includes high melting point metal such as copper to prevent separation of the filler and the resin by the melting of all of the metal filler. ¶ 0024.

Matsumoto advises that it is preferable to use (1) a "metal filler" having a high melting point and (2) a metal having a melting point which can be melted at a melting temperature of the matrix resin. The "metal" may be a single metal of either high melting point or low melting point, or a composite of a single metal or metal alloy such as a copper and tin system alloy (Sn—Cu system alloy).[2] ¶ 0025.

The type of filler to be dispersed in the matrix resin is not limited, *as long as the filler possesses electrical conductivity*. According to Matsumoto, it is preferable that the filler be in the form of a powder or *fiber*, particularly a metal powder. Matsumoto therefore describes a preference for a powder over a fiber. ¶ 0061.

The filler agent forms a *net structure* in the matrix resin. The weight

[2] For a description of a Sn—Cu system alloy, *see* Saunders et al., *The Cu-Sn (Copper-Tin) System, Bulletin of Alloy Phase Diagrams*, Vol., 11 No. 3, pages 278-287 (1990) (copy attached).

of the filler or filler agent may be chosen so that the *net structure* is capable of allowing the flow of necessary electric current. ¶ 0026. We understand "weight" to mean "weight percentage."

When co-injection molding is used to make the material, it is preferable to use resin materials having good injection molding performance. Examples of suitable insulating resin materials include inter alia the following: thermoplastic materials; polybutylene terephthalate (PBT), polyethylene terephthalate PET), ABS resin, polystyrene, polyamide, polyethylene, polypropylene, and polycarbonate. ¶ 0056.

Possible materials for forming the electrically conductive resin material include a resin having the conductivity imparted to it by adding a certain amount of conductive material (filler) to the electrically insulated polymer (matrix resin) to form a three dimensional metal *net structure* in the filler. ¶ 0059.

The "rate of mixture" of the filler and the matrix resin should be controlled to reduce the volume resistance of the generated electrically conductive resin. ¶ 0062. By "rate of mixture," we understand Matsumoto to be addressing the weight percent of filler and matrix resin.

Matsumoto states that the amount of the filler should be relatively small because the more filler, the less mechanical performance of the generated resin. As an example, the Sn—Cu—Ni—P[3] alloy of 50 weight % to 95 weight % can be added to PBT. ¶ 0063. To state that an amount of 50-95 weight % is *small* seems

[3] We believe Matsumoto intended to describe Pb (lead) and not phosphorus (P).

a bit unusual. However, in context, what Matsumoto means becomes clear on consideration of Embodiment 1, to which we now turn.

Matsumoto Figs. 3(a), 3(b) and 4, reproduced below, will assist the reader in understanding Embodiment 1.

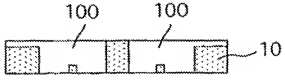

Matsumoto Fig. 3(a)

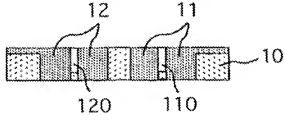

Matsumoto Fig. 3(b)

Figures 3(a) and. 3(b), are schematic illustrations of a procedure for co-injection molding of the case;

FIG. 4

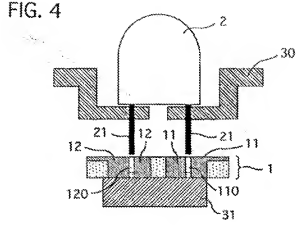

Matsumoto Fig. 4

Fig. 4 is a cross-sectional view of an electrically conductive plastic material and a metal material illustrating a connecting method

With reference to Matsumoto Figs. 3(a), 3(b) and 4, Embodiment 1 describes case body **10** to be used as the insulating portion was formed from insulated thermoplastic resin (PBT resin) as shown in FIG. 3(a) by injection molding, resulting in case body **10** having spaces **100**. After formation of the case body **10**, the case body was again disposed in a die and an electrically conductive resin ((1) Sn—Cu system alloy: 90 weight %; (2) PBT resin: 10 weight %) was injected into the space **100** to form circuits (thickness: 3 mm) by electrically conductive portions **11**, **12** as shown in FIG. 3(b). The combination of the insulative portion **10** and the electrically conductive portions **11**, **12** form the case **1** as shown in Fig. 4. ¶ 0077

In electrically conductive portions **11**, **12**, several connecting holes

110, **120** (diameter: 0.4; depth: 2 mm) were formed during the injection molding for receiving the connecting leads **21** (diameter: 0.5 mm) of light-emitting diodes (LED) **2** as shown in FIG. 4. The leads **21** of the LED 2 are made of phosphor-bronze and are tin-plated on their surface. ¶ 0078.

Embodiment 1 reveals an object of the Matsumoto invention which is to make an electrically conductive plastic material used in an electrical circuit where an LED can be inserted to complete the circuit. See, e.g., ¶¶ 0002 and 0017-0018.

Matsumoto also describes comparative examples, including Comparative Example 2. ¶¶ 102-104.

Case body **10** having an insulated portion was formed as shown in Fig. 2 (we believe Matsumoto intended to refer to Figs. 3(a) and 3(b)) using insulating PBT resin. Case body **10** was again disposed in a die and an electrically conductive resin ((1) PBT resin: 50 weight %; (2) copper fiber: 50 weight %) was injected into the space **100** to form circuits as electrically conductive portions **11**, **12**. Case **1** comprises insulative portions **10** and electrically conductive portions **11**, **12**.

In the electrically conductive portions **11**, **12**, connecting holes **110**, **120** were formed for connecting the LED **2** to leads **21** as in Embodiment 1.

Matsumoto describes heat impact test results in Table 1. ¶ 0111. According to Matsumoto, the Embodiments of the Matsumoto invention "have superior heat impact resistance and high reliability of electric connection" vis-à-vis the Comparison Embodiments.

Nakazawa

Nakazawa describes an electroconductive resin composition comprising:

(A) 30-98 wt% of a thermoplastic resin

(B) 1-50 wt% of an electroconductive fiber, such as a copper fiber; and

(C) 0.1-30 wt% of a low-melting point metal, such as an In—Sn alloy or an In—Bi alloy.

See (1) Abstract (57) and (2) page 3 of 8.[4]

Unlike Matsumoto, Nakazawa was looking for an electroconductive resin which has electromagnetic wave shield properties. *See* (1) Abstract (57) and (2) page 2 of 8.

Kosuga

Kosuga was cited by the Examiner to establish that copper fibers having the claimed dimensions were known to be used in resins to make an electroconductive resin. Answer, page 5.

[4] In ¶ 0009:2, Nakazawa uses the language "which do not contain". In context the language is not clear, no doubt due to the fact that Nakazawa is based on a machine translation. What we think Nakazawa intended to say by the language "which do not contain" is that its composition should, or does, not contain lead (Pb).

Level of skill in the art

We find that the level of skill in the art is high.

One skilled in the art would have recognized or known that:

[1] any conductive particles in the resin should be in contact, one with the other (Specification, ¶ 0003);

[2] the best way of realizing a conducting network in a plastic is to incorporate metal or carbon fibers (Specification, ¶ 0003);

[3] the proportion of the fiber needed is a function of the length of the fiber (Specification, ¶ 0003);

[4] as the length of the fiber increases, processing becomes more problematic (Specification, ¶ 0003);

[5] when shorter fibers are used, resins having a higher proportion by weight of fibers can still be processed by injection molding, but the specific volume resistance remains the same as when longer fibers are used (Specification, ¶ 0003);

[6] fiber networks in resins can result in interruption of electrical conductivity dependent on different coefficients of expansion of the resin and filler (Specification, ¶ 0003);

[7] in Matsumoto's environment, use of a fiber (as opposed to a powder) in a resin may lead to anisotropy when the resin is subjected to injection molding (Matsumoto ¶ 0023);

[8] a high melting point metal is preferably used in combination with a filler (e.g., the electroconductive material in the resin) to prevent separation of the filler and the matrix resin (Matsumoto ¶ 0024);

[9] in Matsumoto's environment, the electroconductive resin preferably has a low volume resistance, such as less than 10^{-2} Ωcm or preferably less than 10^{-4} Ωcm (Matsumoto, ¶ 0058);

[10] in Matsumoto's environment, the type of filler to be dispersed in the resin is not limited as long as the filler possesses electrical conductivity (Matsumoto, ¶ 0061); and

[11] the "rate of mixture" (i.e., weight percent of ingredients) should be controlled to reduce the volume resistance of the conductive resin (Matsumoto, ¶ 0062).

Differences between claimed subject matter and Matsumoto

Difference 1: Siemens maintains that Matsumoto does not describe a "fiber network" (Claims 9 and 19). Appeal Brief, page 9.

Difference 2: Matsumoto does not explicitly describe the *dimensions* of the copper fiber (Claim 9). Answer, page 5:5.

Difference 3: With respect to its invention, Matsumoto does not explicitly describe the use of *copper fibers* in an amount of 30-70% by weight (Claims 9, 16 and 19). Answer, page 5:4.

Difference 4: Matsumoto does not explicitly describe the use of "the components of the ... claimed low melting point metal compound" or *a combination* of copper fibers and low melting metal *in amount ≥ 60% by weight* (Claims 9, 16 and 19). Answer, page 5:3-5, and Appeal Brief, page 9.

Discussion

Difference 1

Matsumoto describes a "fiber network."

Matsumoto describes the use of fibers (even if use of fibers is not preferred) and explicitly states that the filler (which may be a fiber) forms a "net structure." ¶ 0023; ¶ 0059.

Siemens and Matsumoto prepare electroconductive resin/filler compositions using similar, if not identical processes, and there is no basis upon which to find, when a fiber is used, that Matsumoto's process does not yield the same fiber network as that said to have been achieved by Siemens.

Difference 2

Of the independent claims, only Claim 9 calls for a copper fiber dimension.

In the Background of the Invention, the Siemens Specification reveals that one skilled in the art knows that processing of a resin/fiber composition is a function of the dimensions of the fiber. Specification, ¶ 0003.

In our view, one skilled in the art would have been able to determine an appropriate fiber size consistent with a desire to maximize processing of the resin/fiber composition

Difference 3

The claims call for 30-70 wt% of copper fiber.

Matsumoto explicitly describes the use of 50-95 wt% filler (which can be a fiber).

The claimed range overlaps with the prior art range.

Siemens has not made out a case that its range achieves an unpredictable result. Cf. *In re Peterson*, 315 F.3d 1325,1329 (Fed. Cir. 2003) (a *prima facie* case of obviousness typically exists when the ranges of a claimed composition overlap the ranges disclosed in the prior art).

Difference 4

In our view, the appeal turns on Difference 4.

This is a close case and we appreciate the effort made by the Examiner to set out a cogent obviousness rationale. But when the prior art is considered *as a whole*, measured against the claimed subject matter *as a whole*, as a matter of law we have difficulty holding that the claimed subject matter would have been obvious.

Siemens maintains that Matsumoto "teaches away" from using copper fibers in combination with a low melting point resin.

To be sure, use of copper fibers does not seem to be Matsumoto's preferred conducting filler.

Nevertheless, use of fibers is described. Therefore, Matsumoto does not "teach away" from the use of fibers.

The use of copper fibers is described in Matsumoto Comparative Embodiment 2—but in that embodiment the amount of resin is higher (50 wt%) than the 10-25 wt% claimed amount of resin. Matsumoto, ¶ 0102.

Matsumoto tells us based on data in Table 1, that impact resistance of Embodiment 1 (1.1 to 1.4) vis-à-vis Comparative Example 2 (440 1370) is "superior." Matsumoto, ¶ 0112.

While we decline to find that "superior" is a proper characterization of the data, we can see there is a difference.

A person skilled in the art could reasonably argue that the comparison is not scientifically valid. In other words, Embodiment 1 describes the use of 90 wt%

Sn—Cu system alloy, whereas Comparative Example 2 uses 50 wt% copper fibers. There is no comparison using the same weight percent of Sn—Cu system alloy and copper fibers. Nevertheless, Matsumoto's results data is consistent with Matsumoto's teaching that use of filler in the form of fibers may generate anisotropy during an injection molding process. ¶ 0023: last sentence.

To fill the gap in Matsumoto, the Examiner turns to Nakazawa.

Nakazawa describes the use in an electroconductive resin matrix of a combination of low melting point metal, copper fibers and a thermoplastic.

However, the amount of thermoplastic is 30-98 wt% whereas the claims on appeal call for 10-25 wt%.

Siemens 10-25 wt% limitation is apparently based on its examples which describe use of from 10 to 25 wt%.

While the level of skill in this art is high, we cannot articulate a sufficient reason for varying from Nakazawa's requirement for at least 30 wt% resin when copper fibers and a low melting point metal are present—particularly in light of Matsumoto's expressed concern about anisotropy. *Cf. KSR Int'l Inc. v. Teleflex Inc.*, 550 U.S. 380, 418 (2007) (there must be some articulated reasoning with some rational underpinning to support obviousness). Accordingly, we are unable to conclude that the prior art, as a whole, renders the claimed 10-25 wt% range within the skill of the art when a combination of copper fibers and low melting point metal is used to make the resin matrix. On this very narrow ground, therefore, we hold that the subject matter of the claims on appeal would not have been obvious.

Decision

Upon consideration of the appeal, and for the reasons given herein, it is

ORDERED that the decision on the Examiner rejecting claims 9, 12, 16-17, 19 and 21-22 is *reversed*.

FURTHER ORDERED that no time period for taking any subsequent action in connection with this appeal may be extended under 37 C.F.R. § 1.136(a)(1)(iv).

REVERSED

ack

Appeal 2011-006178
Application 10/582,215

Attachment 1

Saunders et al., *The Cu-Sn (Copper-Tin) System, Bulletin of Alloy Phase Diagrams*, Vol., 11 No. 3, pages 278-287 (1990)

34Wil: W.H. Willot and E.J. Evans, "X-Ray Investigation of the Arsenic-Tin System of Alloys," *Philos. Mag., 18*, 114-128 (1934). (Equi Diagram, Crys Structure; Experimental)

35Hag: G. Hagg and A.G. Hybinette, "X-Ray Studies on the Systems Tin-Antimony and Tin-Arsenic," *Philos. Mag., 20*, 913-929 (1935). (Equi Diagram, Crys Structure; Experimental)

65Uga: Y.A. Ugai, Y.P. Zavalsky, V.A. Ugai, S.A. Mostovaya, and L.A. Bityutakaya, "Tin Arsenide: New Intermetallic Semiconductor," *Dokl. Akad. Nauk SSSR, 163*(3), 663-666 (1965) in Russian. (Equi Diagram; Experimental)

66Pan: M.B. Panish, "The Gallium-Arsenic-Tin and Gallium-Arsenic-Germanium Systems," *J. Less Common Met., 10*, 415-424 (1966). (Equi Diagram; Experimental)

***68Eck:** P. Eckerlin and W. Kischio, "Preparation and Crystal Structure of Tin Arsenide (Sn_4As_3) and Tin Phosphide (Sn_4P_3) Phases," *Z. Anorg. Allg. Chem., 363*, 1-9 (1968) in German. (Equi Diagram, Crys Structure; Experimental)

***69Per:** E.A. Peretti and J.K. Paulsen, "Contribution to the System Tin-Arsenic," *J. Less-Common Met., 17*, 283-290 (1969). (Equi Diagram; Experimental; #)

***73Pre:** B. Predel and A. Emam, "Thermodynamic Study of Liquid Binary Alloys of Arsenic with Tin and Thallium," *Z. Metallkd., 64*(10), 689-695 (1973) in German. (Thermo; Experimental)

74Vdo: T.Z. Vdovina and Z.S. Medvedeva, "Phase Diagram of the Tin-Tin Arsenide System," *Zh. Neorg. Khim., 19*(8), 2257-2260 (1974) in Russian. (Equi Diagram, Crys Structure; Experimental; #)

75Dem: A.F. Demidenko, V.I. Koschenko, T.Z. Vdovina, and Z.S. Medvedeva, "Some Properties of Tin Arsenides," *Zh. Neorg. Khim., 20*, 2682-2685 (1975) in Russian. (Equi Diagram, Thermo; Experimental)

***77Zal:** E. Zaleska, "Thermodynamic Properties of Tin-Arsenic Solid Alloys," *Roczn. Chem., 51*(5), 849-853 (1977). (Thermo; Experimental)

78Gla: N.F. Gladyshev and E.A. Pashkov, "Study of Thermodynamic Properties of Intermediate Phases in the Tin-Arsenic System by the Electromotive Force Method," *Fiz. Khim. Poluprovod. Materialoved*, Voronezh, 118-122 (1978) in Russian. (Thermo; Experimental)

82Pan: L.B. Pankratz, "Thermodynamic Properties of Elements and Oxides," Bureau of Mines Bull. 672, 509 (1982). (Thermo; Compilation)

84Pan: L.B. Pankratz, J.M. Stuve, and N.A. Gokcen, "Thermodynamic Data for Mineral Technology," Bureau of Mines Bull. 677, 355 (1984). (Thermo; Compilation)

86Gok: N.A. Gokcen, *Statistical Thermodynamics of Alloys*, Plenum Press, New York, 326 p (1986). (Thermo; Theory)

89Gok: N.A. Gokcen, "The As (Arsenic) System," *Bull. Alloy Phase Diagrams, 10*(1), 11-22 (1989). (Equi Diagram, Thermo; Review)

*Indicates key paper.

#Indicates presence of a phase diagram.

As-Sn evaluation contributed by N.A. Gokcen, 440 East Thornton Lake Dr., Albany, OR 97321. This work was partly supported by ASM INTERNATIONAL. Dr. Gokcen is the ASM/NIST Data Program Category Editor for binary manganese, lead, and silicon alloys.

The Cu-Sn (Copper-Tin) System

By N. Saunders and A.P. Miodownik
University of Surrey
United Kingdom

Equilibrium Diagram

The assessed Cu-Sn phase diagram of Cu-Sn (Fig. 1) is taken from the review of [44Ray]; this diagram is based on extensive work and has stood the test of time. (For a more complete list of references to early work, see [Hansen]; [80BAP] also summarized the data then available.) The system is characterized by a series of peritectic reactions and the formation of a number of ordered, intermetallic phases. This evaluation expands on the abovementioned work with regard to the occurrence of several metastable phases, including martensitic and other

Table 1 Temperature-Invariant Reactions in the Cu-Sn System

Reaction	Composition, at.% Sn		Temperature, °C	Reaction type
(Cu) + L ⇔ β 7.7	15.5	13.1	798	Peritectic
β + L ⇔ γ 15.8	19.1	16.5	755	Peritectic
$\varepsilon \Leftrightarrow \gamma$	25.0		676	Congruent
$\gamma + \varepsilon \Leftrightarrow \zeta$ 21.8	24.5	22.5	640	Peritectoid
$\gamma \Leftrightarrow \varepsilon$ + L 27.9	25.9	43.1	640	Metatectic
$\gamma + \zeta \Leftrightarrow \delta$ 19.8	20.9	20.3	590	Peritectoid
$\beta \Leftrightarrow \alpha + \gamma$ 14.9	9.1	15.4	586	Eutectoid
$\zeta \Leftrightarrow \delta + \varepsilon$ 21.7	20.8	24.5	582	Eutectoid
$\gamma \Leftrightarrow \alpha + \delta$ 16.5	9.1	20.4	520	Eutectoid
ε + L ⇔ η 24.9	86.7	43.5	415	Peritectic
$\delta \Leftrightarrow \alpha + \varepsilon$ 20.5	6.2	24.5	350	Eutectoid
L ⇔ η + (βSn) 98.7	45.5	>99.9	227	Eutectic

structures. Temperature-invariant reactions in the Cu-Sn system are given in Table 1.

Stable Phases

Both the fcc ($cF4$) (Cu) or α phase and bcc ($cI2$) β phase dissolve substantial quantities of Sn. The DO_3 ($cF16$) γ phase also has a wide range of solubility; it is formed by ordering of the β phase [Pearson1]. The structure of the δ phase is cubic ($cF416$) with 413 atoms per unit cell and can be considered as a γ-brass type superstructure, where ordering prevents any close contact between Sn atoms [77Boo]. The ζ phase is hexagonal ($hP26$) and is a superstructure based on the ζAgZn prototype [75Bra]. The

Fig. 1 Assessed Cu-Sn Phase Diagram

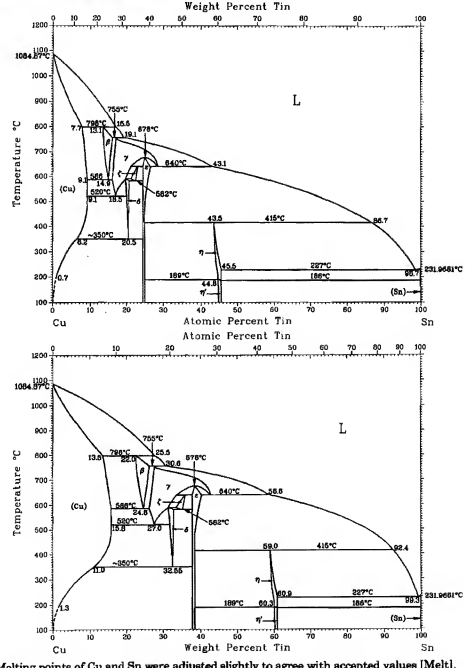

From [44Ray]. Melting points of Cu and Sn were adjusted slightly to agree with accepted values [Melt].

N. Saunders and A.P. Miodownik, 1990.

structure of the ε phase is orthorhombic, ($oC80$) [83Wan]. The basic lattice is of the orthorhombic Cu_3Ti type, with antiphase shifts occurring at every five unit cells along the b_0-axis. Since the basic Cu_3Ti-type structure is itself regarded as a superstructure based on the cph $A3$ lattice, Cu_3Sn belongs to a family of cph-lattice based antiphase structures [83Wan]. η' is hexagonal and is a superstructure based on the NiAs-type structure ($hP4$). On heating it transforms to η between 186 and 189 °C and has the conventional NiAs ($hP4$) structure [73Gan]. The crystal structure of Sn at high temperatures is bct ($tI4$), which transforms at 13 °C under equilibrium conditions and at 1 bar to the diamond cubic structure ($cF8$). The solubility of Cu in (Sn) was reported to be 0.01 at.% Cu [39Hom].

Metastable Phases

Martensite Structures

A major area of interest in Cu-Sn metastable phases concerns the martensite structures that are formed on quenching from the high-temperature β and γ phases. Three types of martensite are usually observed—β_1', β_1'' and γ_1'. The nomenclature for the types of martensite derives from the parent phases, their states of order, and the structure types of the martensitic products before the lattice invariant strain is taken into account. The description and sequence of martensites with composition given below are taken from [72Ken] and [74War].

The β_1' ($18R$) martensite has an ordered orthorhombic structure and is found between 13 and 13.8 at.% Sn. During the quench, the high-temperature β phase orders to the $D0_3$ ($cF16$) structure before the martensite transformation and, therefore, β_1' martensite inherits this order. β_1''($18R/2H$) martensite, found between 13.8 and 15 at.% Sn, is a lamellar composite of orthorhombic β_1' and hexagonal γ_1' martensites, with a composition-dependent orthorhombic distortion arising from a need to minimize transformation stresses. γ_1' martensite, formed by itself between 15 and 15.8 at.% Sn, is a twinned cph structure whose order is inherited from the $D0_3$ ($cF16$) parent phase. There was also a report that it is possible to extend

Table 2 Cu-Sn Crystal Structure Data (Stable Phases)

Phase	Composition, at.% Sn	Pearson symbol	Space group	Strukturbericht designation	Prototype
(Cu)	0 to 9.1	$cF4$	$Fm\bar{3}m$	$A1$	Cu
β	13.1 to 16.5	$cI2$	$Im\bar{3}m$	$A2$	W
γ	15.5 to 27.5	$cF16$	$Fm\bar{3}m$	$D0_3$	BiF_3
δ	20 to 21	$cF416$	$F\bar{4}3m$	...	$Cu_{41}Sn_{11}$
ζ	20.3 to 22.5	$hP26$	$P6_3$	...	$Cu_{10}Sn_3$
ε	24.5 to 25.9	$oC80$	$Cmcm$	...	Cu_3Sn
η	43.5 to 44.5	$hP4$	$P6_3/mmc$	$B8_1$	NiAs
η'	45	(a)	...	...	...
βSn(b)	100	$tI4$	$I4_1/amd$	$A5$	βSn
αSn(c)	100	$cF8$	$Fd\bar{3}m$	$A4$	C(diamond)

Notes: See "Stable Phases" section for references.
(a) Hexagonal; superlattice based on NiAs-type structure. (b) From 13 to 231.9681 °C. (c) Up to <13 °C.

Table 3 Cu-Sn Lattice Parameter Data (Stable Phases)

Phase	Composition, at.% Sn	Lattice parameters, nm a	b	c
(Cu)	0 to 9.1	0.36148 to 0.37046	...	...
β	13.4 to 15.7	0.29781 to 0.29871	...	...
γ	16.6 to 25.0	0.60605 to 0.61176(a)	...	...
δ	20.5	1.7980	...	...
ζ	23.1	0.7330	...	0.7864
ε	25	0.5529	4.7750	0.4323
η	45.45	0.4190	...	0.5086
η'	45.45	2.0870	...	2.5081
βSn	100	0.58315	...	0.31814
αSn	100	0.64892	...	...

From [Pearson3]. (a) At 710 °C.

Table 4 Cu-Sn Crystal Structure Data (Metastable Phases)

Phase	Composition, at.% Sn	Pearson symbol	Space group	Strukturbericht designation	Prototype	Reference
α'	~8 to11.5	*hP*2	$P6_3/mmc$	*A*3	Mg	[63Der, 84Sau]
ω	15 to 16	*hP*12	...	...	...	[81Zak]
X or L	~15	*hP*9	...	...	...	[32Isa, 57Bag, 83Kuw]
β_2	15.5	(a)	...	...	...	[81Zak]
γ'	19.5	(b)	...	...	...	[84Sau]
β'	13 to 16.2	...	4*H*(c)	...	...	[72Ken]
β_1'	13 to 13.8	(d)	18*R*(c)	...	...	[72Ken]
β_1''	13.8 to 15	...	18*R*/2*H*(c)	...	...	[74War]
γ_1'	15 to 15.8	...	2*H*(c)	...	...	[72Ken]
	25					[66Kno]

(a)Ordered rhombic structure. (b)Ordered cubic. (c)Warlimont designation. (d)See text under "Martensite Structures."

Table 5 Cu-Sn Lattice Parameter Data (Metastable Phases)

Phase	Composition, at.% Sn	Lattice parameters, nm *a*	*b*	*c*	Reference
α'	~8	0.261	...	0.427	[63Der]
	11.5	0.263	...	0.427	[84Sau]
ω	15 to 16	0.421	...	1.110	[81Zak]
X	~15	0.728	...	0.258	[32Isa, 57Bag]
L	15	0.740	...	0.260	[83Kuw]
γ_1'	~15	0.456	0.537	0.432	[72Ken]
β_2	15.5	1.273	0.424	0.600	[81Zak]
γ'	19.5	0.899	...	...	[84Sau]

Fig. 2 Lattice Parameter of fcc (Cu) Solid Solution

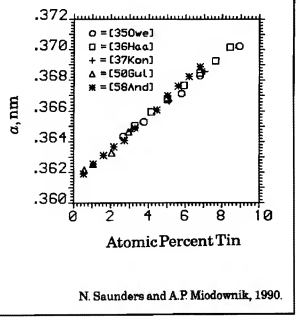

N. Saunders and A.P. Miodownik, 1990.

Fig. 3 Lattice Parameter of bcc (β) Solid Solution

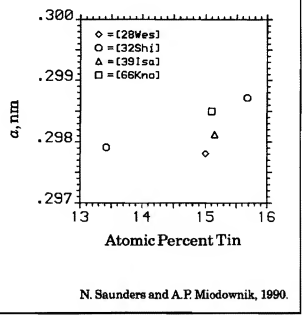

N. Saunders and A.P. Miodownik, 1990.

the range of β_1' martensite to 11.8 at.% Sn by rapid quenching from the melt [70Van].

Between 16 and 25 at.% Sn, the martensite start temperature (M_s) falls sharply and, at compositions greater than 16 at.% Sn, to so far below room temperature that the martensitic transformation is prevented and the DO_3 γ phase is retained. However, the γ_1' martensite is observed again at ~25 at.% Sn; this makes the Cu-Sn system unique in that the γ_1' martensite is observed in two composition ranges. Another martensite β' ($4H$) with an ordered but faulted orthorhombic structure has also been reported [68Nia, 72Ken]. This martensite is observed between 13 and 16.2 at.% Sn when quenched from above some minimum temperature and does not form part of the β_1'-β_1''-γ_1' sequence. The γ_1' martensite, at ~15 to 16 at.% Sn, exhibits thermoelastic behavior [75Miu].

Table 6 Measured Activities of Sn in Liquid Cu-Sn Alloys

Reference	Temperature, K	Composition, mole fraction of Sn	Activity Sn	Activity Cu
[84Ono](a)	1573	0.1	0.02	0.856
		0.2	0.082	0.678
		0.3	0.22	0.498
		0.4	0.373	0.373
		0.5	0.499	0.297
		0.6	0.614	0.227
		0.7	0.712	0.17
		0.8	0.811	0.113
		0.9	0.905	0.064
[72Ois](a)	1373	0.1	0.1	...
		0.2	0.055	...
		0.3	0.198	...
		0.4	0.307	...
		0.5	0.466	...
		0.65	0.652	...
		0.8	0.808	...
		0.9	0.919	...
[78Sen]	1073	0.1	0.007	...
		0.2	0.055	...
		0.3	0.214	...
		0.4	0.353	...
		0.5	0.474	...
		0.6	0.575	...
		0.7	0.683	...
		0.8	0.805	...
		0.9	0.903	...

(a) Digitized from figure in original paper.

Other Phases Observed in Quenched and Aged β and γ Alloys

Numerous other metastable products of quenched and aged β and γ alloys have been reported. The unambiguous crystallographic identification of the products is not always straightforward and can be hampered by the size and distribution of the various phases. It appears fairly certain that at least two phases not observed in the equilibrium phase diagram—the ω and α'— can form in quenched or aged β and γ alloys.

The ω phase reported in alloys quenched from the γ phase [71Van, 73Van, 81Zak] is usually observed as a fine-scale precipitation within the matrix γ phase. The ω phase is associated more commonly with Ti- and Zr-based alloys where the parent phase has the bcc ($cI2$) structure; in this case the structure is hexagonal, with $c/a = 0.63$ [69Sas]. However, in Cu-Sn, ω forms from the DO_3 structure and should theoretically inherit the order of the parent phase [76Pra], with the c-axis quadrupling. Ordering of the ω phase was suggested by the experimental study of [73Van] and subsequently confirmed by [80Zak]. Electron diffraction spots consistent with ω phase reflections were also observed by [83Kuw] from finely dispersed precipitates in a quenched 15 at.% Sn shape-memory alloy. However, as they were not able to ascertain with complete certainty that the phase was ω, they designated it an "s"-phase.

The metastable phase, α', has been observed in both quenched and aged β and γ phase alloys [63Der, 67Deb, 73Van]. [63Der], using X-ray diffraction (XRD), described this phase as straightforward cph ($hP2$) with a composition of ~8 at.% Sn. Later work [67Deb], using thin foils and electron microscopy, suggested that this phase might also be described as a very highly faulted fcc ($cF4$) structure with a stacking fault density of ~0.5.

Table 7 Recommended Integral Thermodynamic Quantities for Liquid Alloys at 1400 K

X_{Sn}	ΔG	ΔH	ΔS	ΔG^{ex}	ΔS^{ex}
0.1	–7 091	–3360	2.655	–3307	–0.038
0.2	–10 607	–4374	4.452	–4782	0.291
0.3	–12 250	–4010	5.886	–5139	0.807
0.4	–12 702	–2996	6.933	–4868	1.337
0.5	–12 345	–1838	7.505	–4277	1.742
0.6	–11 368	–857	7.508	–3534	1.912
0.7	–9 824	–210	6.867	–2713	1.788
0.8	–7 662	79	5.529	–1837	1.368
0.9	–4 702	94	3.426	–918	0.723

Note: Values in J/mol or J/mol·K.

Table 8 Recommended Partial Molar Thermodynamic Quantities for Liquid Alloys at 1400 K

x_{Cu}	a_{Cu}	γ_{Cu}	ΔG_{Cu} J/mol	ΔG^{ex}_{Cu} J/mol	ΔH_{Cu} J/mol	ΔS_{Cu}	ΔS^{ex}_{Cu} J/mol·K
Cu component		**Cu(L) = Cu(in alloy)(L)**					
1.0	1.000	1.000	0	0	0	0.000	0.000
0.9	0.822	0.913	−2 282	−1055	−1356	0.661	−0.215
0.8	0.611	0.763	−5 744	−3146	−4004	1.243	−0.612
0.7	0.448	0.640	−9 356	−5204	−6384	2.123	−0.843
0.6	0.336	0.560	−12 693	−6747	−7614	−3.628	−0.619
0.5	0.258	0.516	−15 777	−7708	−7379	5.999	0.235
0.4	0.197	0.492	−18 929	−8262	−5825	9.360	1.742
0.3	0.143	0.475	−22 674	−8658	−3444	13.736	3.725
0.2	0.092	0.460	−27 780	−9044	−967	19.152	5.770
0.1	0.045	0.450	−36 100	−9294	−744	26.317	7.172
0.0	0.000	0.468	∞	−8842	806	∞	6.891

x_{Sn}	a_{Sn}	γ_{Sn}	ΔG_{Sn} J/mol	ΔG^{ex}_{Sn} J/mol	ΔH_{Sn} J/mol	ΔS_{Sn}	ΔS^{ex}_{Sn} J/mol·K
Sn component		**Sn(L) = Sn(in alloy)(L)**					
0.0	0.000	0.021	∞	−45 239	−49 228	∞	−2.849
0.1	0.013	0.132	−50 370	−23 564	−21 394	20.697	1.552
0.2	0.076	0.378	−30 058	−11 322	−5 854	17.289	3.907
0.3	0.196	0.652	−19 002	−4 986	1 526	14.663	4.652
0.4	0.336	0.839	−12 716	−2 049	3 930	11.890	4.272
0.5	0.465	0.930	−8 913	−844	3 704	9.012	3.249
0.6	0.581	0.968	−6 326	−380	2 455	6.272	2.025
0.7	0.690	0.986	−4 316	−164	1 176	3.923	0.957
0.8	0.798	0.997	−2 633	−35	341	2.124	0.269
0.9	0.901	1.001	−1 213	13	22	0.882	0.006
1.0	1.000	1.000	0	0	0	0.000	0.000

Fig. 4 Lattice Parameter of $D0_3$ (γ) Solid Solution at 605 and 710 °C

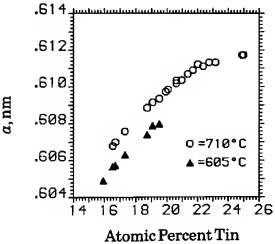

From [66Kno]. N. Saunders and A.P. Miodownik, 1990.

Fig. 5 Experimental Enthalpy of Mixing Data for Liquid Cu-Sn Alloys

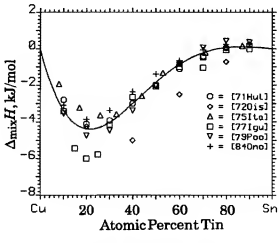

— ≡ recommended values. Values of [79Poo] represent an optimized fit of their experimental results.
N. Saunders and A.P. Miodownik, 1990.

Table 9 Recommended Enthalpies of Formation of Solid and Liquid Alloys at 723 K

$(1-x)Cu(s) + xSn(s) = Cu_{(1-x)}Sn_x(s)$
$(1-x)Cu(L) + xSn(L) = Cu_{(1-x)}Sn_x(L)$

x_{Sn}	Phase	ΔH	x_{Sn}	Phase	ΔH
0.090(a)	(Cu)	−1165	0.825(a)	L	−671
0.205	δ	−5350	0.85	L	−515
0.240	ε	−7650	0.90	L	−263
0.435	η	−7030(b)	0.95	L	−104

From [56Kle1], [56Kle2], and [73Gan]. (a) Phase boundary. (b) ΔH at 237 K.

Table 10 Recommended Partial Gibbs Energy of Sn in Solid Alloys at 1000 K

x_{Sn}	Phase	ΔG_{Sn}, J/mol
0.008	(Cu)	−54 350
0.012	(Cu)	−50 354
0.021	(Cu)	−45 606
0.043	(Cu)	−38 618
0.069	(Cu)	−33 600

From [74Alc]. Data given relative to pure liquid Sn.

[34Isa] and [34Bug] observed an intermediate phase "X" on tempering a quenched γ phase alloy whose structure they identified as either tetragonal or hexagonal, isomorphous with the ζ AgZn structure. Later work [57Bag] confirmed that the diffraction pattern is more consistent with that of the hexagonal structure and therefore "X" is closely related to the ζ equilibrium phase. [83Kuw] identified an "I" phase in a 15 at.% Sn shape-memory alloy. The phase appears to be the same as that described by [57Bag].

ζ phase itself has been observed on annealing quenched, 16.5 at.% Sn γ phase alloys at 300 °C [63Der, 67Deb]. It coexists with the metastable α' phase (see above) and the equilibrium δ and α phases before final decomposition to the equilibrium two-phase structure of $\alpha + \varepsilon$. The ζ or δ phases appear either separately or together, depending on the specimen size and its previous thermal and mechanical history [67Deb]. The formation of these metastable aging products was considered to be caused by the alloys adopting metastable equilibria, which are energetically favorable under limited kinetic conditions [63Der]. Other reported decomposition products of quenched and aged alloys include an ordered orthorhombic (β_2) phase [67Mor, 81Zak] and a δ' phase, which was considered an intermediate structure between ω and the equilibrium δ phase [73Van].

Phases Formed on Vapor Quenching

A series of metastable structures have been reported on vapor quenching of alloys of 11.5 and 19.5 at.% Sn, with the occurrence of the various phases controlled by the composition and substrate temperature [84Sau, 85Sau, 87Sau1]. Below 200 °C, a cph ($hP2$) phase, denoted α', and a cubic phase, γ', were observed. The α' phase, observed at 11.5 at.% Sn, is probably equivalent to the phases found in earlier studies of quenched β and γ phase alloys [63Der, 67Deb, 73Van]. On deposition at room temperature, only cph ($hP2$) lines were observed with XRD. However, depositing at ~130 °C produced a pattern containing both fcc ($cF4$) and cph ($hP2$) lines. The cubic γ' phase (a = 0.899 nm) observed at 19.5 at.% Sn, was considered [84Sau, 87Sau1] to be isomorphous with the more usual γ-brass structures observed in Cu alloys [Pearson1]. At ~200 and ~300 °C, 19.5 at.% Sn alloys contained primarily the ζ phase, whereas 11.5 at.% Sn alloys contained a mixture of ζ and supersaturated α. The occurrence of the above structures was considered to be due to the alloys adopting a series of low-temperature metastable equilibria, limited by kinetics at the surface of the film during deposition [84Sau, 85Sau, 87Sau1] (see also [63Der]).

Amorphous phases have been observed on vapor codeposition at very low temperatures (< 77 K) in a 90 at.% Sn alloys [54Buc], at 77 K in a 60 at.% Sn alloy [68Cho], and between ~30 and 80 at.% Sn at 4.2 K [83Hau]. A metastable phase was reported to form on annealing of thin-layered structures produced by the sequential vapor deposition of pure Cu and Sn [61Mit, 79She]. From its electron diffraction pattern, the structure was postulated to be diamond cubic, with a = 1.734 nm. However, such a structure is highly unlikely and was not reported [Pearson3] in other Cu alloys.

Crystal Structures and Lattice Parameters

Tables 2 and 3 summarize crystal structure and lattice parameter data for the equilibrium system, whereas Tables 4 and 5 provide these data for the metastable phases. Figures 2 and 3 show the lattice parameter vs composition measurements for the (Cu) and β phases from various authors where there is fairly good agreement between the studies. [66Kno] measured the lattice parameter variation of the DO_3 γ phase with composition of 605 and 710 °C which is shown in Fig. 4.

Thermodynamics

[71Hul] reviewed the literature prior to 1970. Since then, a number of experimental studies have been reported. Activities of liquid alloys were measured by [72Ois], [78Ser], and [84Ono] (Table 6). All of these reports are in broad agreement with [71Hul]. However, they do suggest that the activity of Sn exhibits a slight positive deviation from ideality in Sn-rich alloys rather than the slightly negative

deviation proposed by [71Hul]. Enthalpies of mixing have been measured calorimetrically [75Ita, 77Igu, 79Poo] and derived from high-temperature activity measurements [72Ois, 84Ono]. These results are for the most part in good agreement with [71Hul] and characteristically show a minimum around ~20 to 30 at.% Sn (Fig. 2). There are two experimental studies of partial Gibbs energies of Sn in the (Cu) phase [72Pre, 74Alc]. The values of [72Pre] are substantially more negative that those of [74Alc]. However, [74Alc] showed that their results are consistent with values derived using measured liquid activities and the known phase diagram; consequently [74Alc] is considered more accurate. [73Gan] measured thermodynamic properties of the η phase.

Recommended values for thermodynamic properties of the Cu-Sn system which take into account these recent values are shown in Tables 6 to 10. Recommended values for the liquid phase were selected using the computer program BINGSS developed by [77Luk]. BINGSS uses a least-squares method to optimize thermodynamic functions based on experimentally measured thermodynamic and phase diagram data. In the present case, only experimentally measured thermodynamic data were used. Values in Table 7 have been transferred to the respective reference states assuming ΔH_m for Cu = 13 054 J/mol [71Hul] and ΔH_m for Sn = 7029 J/mol [Hultgren,E].

Due to the complexity of the ordered phase equilibria, thermodynamic phase diagram calculations have been very limited. A reasonable fit with the phase diagram has been achieved [84Sau] (see also [85Mio]). However, it was not possible to fit the ordered phases γ and ζ using a conventional treatment such as the Bragg-Williams model. Instead, it was necessary to add a small parabolic Gibbs energy contribution, tentatively associated with electronic effects and confined within empirically evaluated composition limits, to a standard subregular model. The approach, although empirical, results in Gibbs energy curves that support the proposed relative stability of the ζ phase at low temperatures and could subsequently be used to explain its appearance as a metastable phase [63Der, 84Sau, 85Sau, 87Sau1] (see "Metastable Phases" section).

Attempts here at calculation of the phase diagram using more sophisticated sublattice modeling [81Sun] have proved unsuccessful. This in itself may be seen as confirming the importance of electronic contributions to the phase stability of the ordered structures as proposed by [85Mio]. However, it is clear that for a completely satisfactory thermodynamic phase diagram calculation, a proper ordering model should necessarily be included in the description for the ordered phases in this system.

The relative stability of the cph (*hP2*) and fcc (*cF4*) structures in Cu-based alloys was analyzed by [87Sau2]. Using reported stacking fault energies of Cu-Sn alloys [70Gal], they were able to show that, at low temperatures, the underlying stability of the cph structure increases with alloying and above ~10 at.% Sn, it becomes more stable than the fcc (*cF4*) structure. This increase in the relative stability of the cph structure on alloying is consistent both with the experimentally observed transition from the fcc-based, β_1' martensite to the cph-based, γ_1' martensite with increasing Sn concentration and the formation of the cph metastable α' phase [63Der, 67Deb, 73Van, 84Sau, 85Sau, 87Sau1] (see "Metastable Phases" section).

Cited References

28Wes: A. Westgren and G. Phragmen, "X-Ray Analysis of Copper-Tin Alloys," *Z. Anorg. Chem.*, *175*, 80-89 (1928). (Equi Diagram, Crys Structure; Experimental)

32Shi: G. Shinoda, "Eutectoid Transformation of Bronze," *Sujokai-Shi*, *7*, 367-372 (1932). (Equi Diagram, Crys Structure; Experimental)

34Isa: I.V. Isaichev and G.V. Kurdyumov, "Transformation in Copper-Tin Eutectoid Alloys I," *Z. Phys.* (USSR) *5*, 26-21 (1932). (Meta Phases, Crys Structure; Experimental)

34Bug: V. Bugakov, I.V. Isaichev, and G.V. Kurdyumov, "Transformation in Copper-Tin Eutectoid Alloys II," *Z. Phys.* (USSR), *5*, 22-30 (1934). (Meta Phases, Crys Structure; Experimental)

35Owe: E.A. Owen and J. Iball, "X-Ray Investigation of the Phase Boundaries of Certain Cu-Sn Alloys," *J. Inst. Met.*, *57*, 267-284 (1935). (Equi Diagram, Crys Structure; Experimental)

36Haa: C. Haase and F. Pawlek, "Copper-Tin Alloys," *Z. Metallkd.*, *28*, 73-86 (1936). (Equi Diagram, Crys Structure; Experimental)

37Kon: S.T. Konobeevskii and W.P. Tarrassova, "The Equilibrium Diagram for the System Cu-Sn and the Transformation Associated with the Decomposition of the Solid Solution α," *Acta. Physiochim. URSS*, *6*, 781-798 (1937). (Equi Diagram, Crys Structure; Experimental)

39Hom: O.E. Homer and H. Plummer, "Embrittlement of Tin at Elevated Temperatures and Its Relationship to Impurities," *J. Inst. Met.*, *64*, 169-200 (1939). (Equi Diagram; Experimental)

39Isa: I. Isaichev, "Transformation in Eutectoid Alloys of Copper and Tin IV: Decomposition of β Phase on Annealing," *Zh. Tekh. Fiz. 9*, 1867-1872 (1939). (Equi Diagram, Crys Structure; Experimental)

44Ray: G.V. Raynor, "The Cu-Sn Phase Diagram," *Annotated Equilibrium Diagram Series*, No. 2, The Institute of Metals, London (1944). (Equi Diagram; Review)

50Gul: A.P. Gulyaev and E.F. Trusova, "Laws of Variation of Properties in Solid Solutions," *Zh. Tekh. Fiz. 20*, 66-82 (1950). (Crys Structure; Experimental)

54Buc: W. Buckel, "Electron Diffraction Photographs of Thin Metal Films at Low Temperatures," *Z. Phys.*, *138*, 136-150 (1954). (Meta Phases, Crys Structure; Experimental)

56Kle1: O.J. Kleppa, "A Calorimetric Investigation of Some Binary and Ternary Liquid Alloys Rich in Tin," *J. Phys. Chem.*, *60*, 842-846 (1956). (Thermo; Experimental)

56Kle2: O.J. Kleppa, "Heat of Formation of Solid and Liquid Binary Alloys of Copper with Cadmium, Indium, Tin and Antimony at 450 °C," *J. Phys. Chem.*, *60*, 852-858 (1956). (Thermo; Experimental)

57Bag: I.A. Bagariatskii, "Crystal Structure of the Metastable Phase Formed During the Tempering of Cu-Sn Alloys Containing 24-27 wt.% Sn," *Sov. Phys. (Crystallogr.)*, *2*, 277-280 (1957). (Meta Phases, Crys Structure; Experimental)

58And: A.F. Anderson, "The Effect of Tin on the Lattice Parameter of Copper," *Trans. Met. Soc. AIME*, *212*, 259-260 (1958). (Crys Structure; Experimental)

61Mit: T. Mitsuishi, "An Electron Diffraction Study on Cu-Sn Alloys," *J. Phys. Soc. Jpn., 16*, 453-455 (1961). (Meta Phases, Crys Structure; Experimental)

63Der: A. Deruyterre, "Phase Transformations Occurring at 300 °C in an Alloy of Copper plus 16.5 at.% Tin," *Mem. Sci. Rev. Metall., 60*, 359-370 (1963). (Meta Phases, Crys Structure, Thermo; Experimental)

66Kno: H. Knodler, "On the Crystal Structure and Structure Relationships of the γ and ε Phases in the Cu-Sn System," *Metall., 20*, 823-829 (1966). (Equi Diagram, Crys Structure; Experimental)

67Mor: H. Morikawa, K. Shimizu, and Z. Nishiyama, "Structure of Quenched β Phase and Its Decomposition Products in Cu-Sn Alloys," *Trans. Jpn. Inst. Met., 8*, 145-152 (1967). (Meta Phases, Crys Structure; Experimental)

67Deb: M. De Bondt and A. Deruyette, "Pearlite and Bainite Formation in a Cu-16.5 at.% Sn Alloy," *Acta Metall., 15*, 993-1005 (1967). (Meta Phases, Crys Structure; Experimental)

68Cho: K.L. Choptra, Ledgemont Lab. report TR-179, August, 1968. (Meta Phases; Experimental)

68Nis: Z. Nishiyama, K. Shimizu, and H. Morikawa, "Electron Microscope Study of the Banded β′ Martensite in a Cu-Sn Alloy," *Trans. Jpn. Inst. Met., 9*, 307-316 (1968). (Meta Phases, Crys Structure; Experimental)

69Sas: S.L. Sass, "The ω Phase in a Zr-25 at.% Ti Alloy," *Acta Metall., 17*, 813-820 (1969). (Meta Phases, Crys Structure; Experimental)

70Gal: P.C.J. Gallagher, "The Influence of Alloying, temperature and Related Effects on the Stacking Fault Energy," *Metall. Trans., 1*, 2429-2461 (1970). (Meta Phases; Review)

70Van: W. Vandermeulen and A. Deruyterre, "Structures Obtained in a Cu-11.8 at.% Sn Alloys Quenched from the Melt," *Fizika, 2*, Suppl. 2, 8.1-8.5 (1970). (Meta Phases, Crys Structure; Experimental)

71Hul: R. Hultgren and P.D. Desai, "Selected Thermodynamic Values and Phase Diagrams for Copper and Some of Its Binary Alloys," *INCRA Monograph on the Metallurgy of Copper*, No. 1, International Copper Research Association, U.S.A. (1971). (Thermo; Review)

71Van: W. Vandermeulen, Ph.D. Thesis, Leuven University, Belgium (1971). (Meta Phases, Crys Structure; Experimental)

72Ken: N.F. Kennon and T.M. Miller, "Martensitic Transformations in β1 Cu-Sn Alloys," *Trans. Jpn. Inst. Met., 13*, 322-326 (1972). (Meta Phases; Review)

72Ois: T. Oishi, T. Hiruma, and J. Moriyama, "Thermodynamic Studies of Molten Cu-Sn Alloys Using Zirconia Solid Electrolytes," *J. Jpn. Inst. Met., 36*, 481-485 (1972). (Thermo; Experimental)

72Pre: B. Predel and U. Schallner, "Thermodynamic Investigation of the Cu-Ga, Cu-In, Cu-Ge and Cu-Sn Systems," *Mater. Sci. Eng., 10*, 249-258 (1972). (Thermo; Experimental)

73Gan: A. Gangulee, G.C. Das, and M.B. Bever, "An X-Ray Diffraction and Calorimetric Investigation of the Compound Cu_6Sn_5," *Metall. Trans., 4*, 2063-2066 (1973). (Thermo; Experimental)

73Van: W. Vandermeulen and A. Deruyterre, "An ω Phase in the Cu-16.5 At. Pct Sn Alloy," *Metall. Trans., 4*, 1659-1664 (1973). (Meta Phases, Crys Structure; Experimental)

74Alc: C.B. Alcock and K.T. Jacob, "Solute-Solute and Solvent-Solute Interactions in α-Solid Solutions of Cu + Sn, Au + Sn, and Cu-Au-Sn Alloys," *Acta Metall., 22*, 539-544 (1974). (Equi Diagram, Thermo; Experimental)

74War: H. Warlimont and L. Delaey, "Martensitic Transformations in Copper, Silver and Gold Based Alloys," *Progr. Mater. Sci., 18*, 1-154 (1974). (Meta Phases; Review)

75Bra: J.K. Brandon, W.B. Pearson, and D.J.N. Tozer, "A Single-Crystal Diffraction Study of the ζ Bronze Structure, $Cu_{39}Sn_8$," *Acta Crystallogr. B, 31*, 774-779 (1975). (Equi Diagram, Crys Structure; Experimental)

75Ita: K. Itagaki and A. Yazawa, "Heats of Mixing in Liquid Copper or Gold Binary Alloys," *Trans. Jpn. INst. Met., 16*, 679-685 (1975). (Thermo; Experimental)

75Miu: S. Miura, Y. Morita, and N. Nakanishi, "Superplasticity and Shape Memory Effect in Cu-Sn Alloys," in "Shape Memory Effects in Alloys," J. Perkins, Ed., Plenum Press, NY, 389-405 (1975). (Meta Phases, Crys Structure; Reiview)

76Pra: A. Prasetyo, F. Reynaud and H. Warlimont, "Elastic Constant Anomalies and Precipitation of an ω Phase in Some Metastable $Cu_{2+x}Mn_{1-x}Al$ b.c.c. Alloys," *Acta Metall., 24*, 651-658 (1976). (Meta Phases, Crys Structure; Experimental)

77Boo: M.H. Booth, J.K. Brandon, R.Y. Brizard, C. Chieh, and W.B. Pearson, "γ-Brasses with F Cells," *Acta Crystallogr. B, 33*, 30-36 (1977). (Equi Diagram, Crys Structure; Experimental)

77Igu: Y. Iguchi, H. Shimoje, S. Ban-Ya, and T. Fuwa, "Calorimetric Study of Heat of Mixing of Cu Alloys at 1120 °C, *Tetsu-to-Hagane, (J. Iron Steel Inst. Jpn.) 63*, 275-284 (1977). (Thermo; Experimental)

77Luk: H. Lukas, E.T. Henig, and B. Zimmermann, "Optimization of Phase Diagrams by a Least-Squares Method Using Simultaneously Different Types of Data," *Calphad, 1*, 225-236 (1977). (Thermo; Theory)

78Sen: A.K. Sengupta, K.P. Jagannathan, and A. Ghosh, "Thermodynamic Measurements in Liquid Cu-Sn Alloys," *Met. Trans. B, 9*, 141-143 (1978). (Thermo; Experimental)

79Poo: M.J. Pool. B, Predel, and E. Schultheiss, "Application of the SETARAM High Temperature Calorimeter for Determination of Mixing Enthalpies of Liquid Alloys," *Thermochim. Acta, 28*, 349 (1979). (Thermo; Experimental)

79She: Y. Shevakin, L. Kharitonova, and L. Ostravskaya, "Dependence of Structure and Properties of Vacuum Condensates of Some Metals and Alloys on Conditions of Deposition," *Thin Solid Films, 62*, 337-346 (1979). (Meta Phases, Crys Structure, Experimental)

80BAP: "The Cu-Sn System," *Bull. Alloy Phase Diagrams, 1*(1), 87-89 (1980). (Equi Diagram; Review)

81Sun: B. Sundman and J. Agren, "A Regular Solution Model for Phases with Several Components and Sublattices Suitable for Computer Applications," *J. Phys. Chem. Solids, 42*, 297-301 (1981). (Thermo; Theory)

81Zak: M.I. Zakharova and G.N. Dudchenko, "Phase Diagram in Quenched and Aged Copper-Tin and Copper-Tin-Aluminum Alloys," *Phys. Met. Metall., 49*, 174-177 (1981). (Meta Phases, Crys Structure; Experimental)

83Hau: P. Haussler and F. Baumann, "The Influence of the Average Electron Concentration on the Properties of Amorphous Tin-Noble Metal Alloys and a Comparison of the Amorphous with Liquid Alloys," *Z. Phys. B, 49*, 303-312 (1983). (Meta Phases; Experimental)

83Kuw: N. Kuwana and C.M. Wayman, "Precipitation Processes in a β-Phase Cu-15 at.% Sn Shape Memory Alloy," *Trans. Jpn. Inst. Met., 24*, 561-573 (1983). (Meta Phases, Crys Structure; Experimental)

83Wat: Y. Watanabe, Y. Fujinaga, and H. Iwasaki, "Lattice Modulation in the Long-Period Superstructure of Cu_3Sn,"

Acta Crystallogr. B, 39, 306-311 (1983). (Equi Diagram, Crys Structure; Experimental)

84Ono: K. Ono, S. Nishi, and T. Oishi, "A Thermodynamic Study of Liquid Cu-Sn and Cu-Cr Alloys by the Knudsen Cell-Mass Filter Combination," *Trans. Jpn. Inst. Met., 25*, 810 (1984). (Thermo; Experimental)

84Sau: N. Saunders, Ph.D. Thesis, "Phase Formation Co-Deposited Alloy Thin Films," Univ. of Surrey, U.K. (1984). (Equi Diagram, Meta Phases, Crys Structure, Thermo; Experimental)

85Mio: A.P. Miodownik, "Progress in Understanding The Cu-Sn Phase Diagram," *J. Less-Common Met., 114*, 81-87 (1985). (Equi Diagram, Meta Phases, Thermo; Review)

85Sau: N. Saunders and A.P. Miodownik, "The Use of Free Energy vs Composition Curves in the Prediction of Phase Formation in Co-Deposited Alloy Films," *Calphad, 9*, 283-290 (1985). (Meta Phases, Crys Structure, Thermo; Theory)

87Sau1: N. Saunders and A.P. Miodownik, "Phase Formation Co-Deposited Metallic Alloy Thin Films," *J. Mater. Sci., 22*, 629-637 (1987). (Equi Diagram, Meta Phases, Crys Structure, Thermo; Experimental)

87Sau2: N. Saunders and A.P. Miodownik, "The Observation of a Non-Equilibrium Close Packed Hexagonal Phase in Alloys of Copper with Group III-IVB Elements," *Calphad, 11*, 159-161 (1987). (Meta Phases, Crys Structure, Thermo; Experimental)

Cu-Sn evaluation contributed by **N. Saunders** and **A.P. Miodownik**, Dept. of Materials Science and Engineering, University of Surrey, Guildford, Surrey GU2 5XH, UK. This work was supported by ASM INTERNATIONAL. Literature searched through 1988. Professor Miodownik is an ASM/NIST Data Program Contributing Editor for binary copper alloys.

The H-Na (Hydrogen-Sodium) System

By A. San-Martin and F.D. Manchester
University of Toronto

Equilibrium Diagram

The temperature-composition diagram* of the Na-H system shown in Fig. 1 consists of the following phases: βNa, the pure bcc form; NaH, with nominal stoichiometry and fcc structure; and (L_1), liquid Na containing absorbed H.

Crystal structure and lattice parameters data for the H-Na system are given in Table 1. For the phase NaH, selected experimental data have been arranged in Table 2 (density), and Tables 3 and 5 (Thermodynamics).

The (L_1)/(L_1) + NaH boundary** in Fig. 1, was calculated with Eq 3 below, which is the assessed analytical approximation for the solubility limit of H in liquid Na (see Fig. 2). The atomic ratio X (X = H/Na) amounts to around 8×10^{-7} (~8×10^{-6} at.% H), at 110 °C, the lowest temperature measured so far [74Vis], and 2×10^{-3} (0.2 at.% H) at 428 °C, the decomposition temperature at 0.1 MPa.

*In metal hydrogen (M-H) systems, the equilibrium pressure of the hydrogen surrounding the metal is always a significant thermodynamic variable, in contrast to most situations involving metallic alloys. Two sections of the P-T-X surface (T-X and P-X diagrams) are therefore necessary. However, for the Na-H system such diagrams are only available at high pressures (see Fig. 3 and 4), and are not readily compatible with Fig. 1. In the presentation given here P is the pressure (in Pascals), T the temperature (in °C), and X the H concentration (expressed as X = H/Na, the atomic ratio).

**Because, as with other alkali metals [68Mag], H is readily bonded, stoichiometrically, with Na, we assume that we can represent the mixed phase field of Fig. 1 by the designation (L_1) + NaH, a practice we have not used for transition metal (M-H) systems because stoichiometric arrangements in them are not often encountered.

The H solubility in liquid Na increases at hydrogen pressures higher than 0.1 MPa. The experimental pressure-composition isotherms reported by [82Klo] (Fig. 3) show that at a pressure of 66.4 MPa and a temperature of 900 °C, the maximum observed solubility of H in liquid Na amounts to X = 0.186 (15.7 at.% H). The maximum solubility values from the isotherms of Fig. 3 delineate in Fig. 4 the boundary between L_1 and the two-phase region comprised of (L_1) and L_2. In the T-X diagram of Fig. 4, for an equilibrium pressure of 250 MPa, the principal features postulated by [82Klo] were preserved. The most probable values for the critical point were estimated by [82Klo] using three different procedures (which includes the method of Kordes [53Kor] and the rectilinear diameter rule) and are:

T_c = 1227 ± 70 °C; X = 0.65 ± 0.05; and p = 250 ± 60 MPa.

The melting point temperature (T_M) of the NaH phase is assessed to be 638.8 °C (at p = 11.25 MPa), derived by the procedure of [82Klo] from a plots of log P vs 1/T with his data as well as with the equilibrium data of [55Ban], [76Sku], and [82Klo]. T_M values derived by [76Sku] and [82Klo] are listed in Table 4.

Solubility of H in Liquid Na

Observations that Na absorbs H were first mentioned by [1811Gay] (cited in [1874Tro1]). [1874Tro1] and [1874Tro2] found that under atmospheric pressure, H was absorbed by Na only up to temperatures of 421 °C, and that a crystalline alloy of Na and H was formed (see NaH phase). These early studies of the H solubility in Na, as well as many others [02Moi, 12Key, 21Eph, 37Sol,

Appeal 2011-006178
Application 10/582,215

Attachment 2

Printout of http://mcpmetspec.thomasnet.com/item/low-melting-point-alloys/mcp200-metspec-390/item-1012

Request Information

Item # Item-1012, MCP200/METSPEC 390

MCP200/METSPEC 390

Please Click Here to request alloys not listed.

Specifications · Physical Properties · Tensile Properties · The Tin-Zinc Phase Diagram · Solidification · Melting · Viscosity · Typical Uses

Specifications

Compressive Properties (Proof stress at 2 days and 70 days)	(0.2% set) 51.8 falling to 50.8 Mpa (1.0% set) 62.4 falling to 58.1 Mpa
Melting Point	197 ºC 390 ºF
Specific Heat	(Solid, 25ºC) 0.238 $J.g^{-1}.ºC^{-1}$ (Liquid, 160ºC) 0.272 $J.g^{-1}.ºC^{-1}$
Density	7.27 $g.mr^{-1}$
Brinell Hardness BS 240: 1986 (1991)	21.5 to 24.5
Latent Heat of Fusion (At Immediate Re-Fusion)	71.2 $J.g^{-1}$
Thermal Conductivity	0.61 $J.sec^{-1}.cm^{-1}.ºC^{-1}$
Electrical Resistivity (0.162x Conductivity of Cu)	11.2 µU.cm

Physical Properties

METSPEC 390 is probably the eutectic of the tin-zinc system, although there is some conflict in the published data.
In common with all alloys of low melting point, Metspec 390 undergoes equilibration after solidification. Although melting behavior depends on the age and thermal history of the alloy, the observed differences are of much less significance than those seen in alloys based on bismuth, which melt within a much lower temperature range, where the changes are slower and usually more complex.
The alloy when molten is susceptible to dross formation through oxidation, and a protective atmosphere is recommended. Pressurized nitrogen is preferable to air as the motive gas in spraying.

MCP HEK GMBH

SIDECH

alumin

Tensile Properties

Data at 2 Days and 70 Days	BS EN 10 020
Modules of Elasticity	
Proof Stress, 0.2% set	48.5 falling to 42.7 MPa
Tensile Strength	64.3 falling to 54.7 MPa
Elongation (% in 5.65 A)	30 rising to 32.5

The Tin-Zinc Phase Diagram

The diagram is based on published data (e.g. M. Hansen & K. Anderko, "Constitution of Binary Alloys"; C.J. Smithells, 'Metals Reference Book').
The eutectic composition (9.0% wt. of zinc) and temperature (197ºC) are values based on measurements made by MCP Ltd.

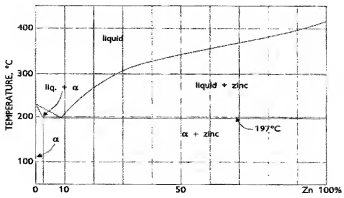

Solidification

The trace obtained by solidification from a homogeneous melt of a sample of 300 g indicates a precise arrest at 197°C, which follows a short supercooling. There is no post-solidification evidence from this diagram of further reaction. For this alloy, the level plateau defines very precisely the eutectic temperature, which may be compared with the onset values found in melting of both newly solidified and matured samples.

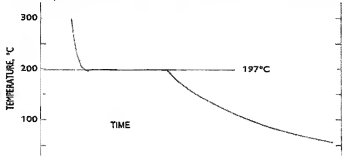

Melting

The minor structural changes that take place after solidification are made apparent by the technique of Differential Scanning Calorimetry (DSC). The behavior of matured alloy is here compared with that of a newly solidified specimen.
The onset temperature for melting is found to have altered slightly in older specimens. The virtual absence of structural changes after solidification is demonstrated by the similarity in melting behavior between specimens of different ages (or which have been subjected to different conditioning).

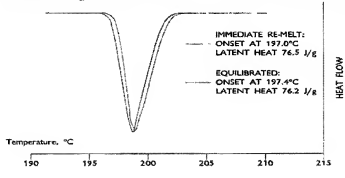

Viscosity

Like that of most alloys of low melting point, the viscosity of METSPEC 390 is quite low and apparently non-Newtonian. However, the data shown are undoubtedly influenced by the circumstances of measurement and, not least, by the high surface tension of the alloy, especially close to its melting point.
The values indicated in the diagram were obtained by means of a Brookfield RVT viscometer, using 3 liters of liquid alloy in a cylindrical container with alloy depth being roughly equal to the diameter. The figure illustrates changes apparent under conditions such as might be encountered in practical use. Viscosity is, in fact, so low that it is not a large consideration in designing systems for circulating large quantities of alloy.

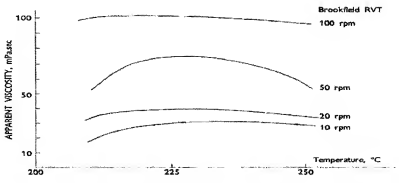

Typical Uses

METSPEC 390 alloy is used almost exclusively in spraying applications. These are mainly based on the MCP range of spray guns, designed for the rapid formation of alloy moulds for plastics such as polyurethanes. The alloy is suitable for thermal protection devices designed to yield at 197°C.

Request Information

MCP Group
515 Commerce Dr.
Fairfield, CT 06432
Phone:203.384.0335 • **Fax:**203.368.4082
E-mail: info@mcp-group.com • **Web site:**www.mcp-group.com

Item # item-1012, MCP200/METSPEC 390

MCP200/METSPEC 390

Please Click Here to request alloys not listed.

· SPECIFICATIONS · PHYSICAL PROPERTIES · TENSILE PROPERTIES · THE TIN-ZINC PHASE DIAGRAM · SOLIDIFICATION · MELTING · VISCOSITY · TYPICAL USES

SPECIFICATIONS

Compressive Properties (Proof stress at 2 days and 70 days)	(0.2% set) 51.8 falling to 50.8 Mpa (1.0% set) 62.4 falling to 58.1 Mpa
Melting Point	197 °C 390 °F
Specific Heat	(Solid, 25°C) 0.239 $J.g^{-1}.°C^{-1}$ (Liquid, 160°C) 0.272 $J.g^{-1}.°C^{-1}$
Density	7.27 $g.ml^{-1}$
Brinell Hardness BS 240: 1986 (1991)	21.5 to 24.5
Latent Heat of Fusion (At Immediate Re-Fusion)	71.2 $J.g^{-1}$
Thermal Conductivity	0.61 $J.sec^{-1}.cm^{-1}.°C^{-1}$
Electrical Resistivity (0.152x Conductivity of Cu)	11.2 µU.cm

PHYSICAL PROPERTIES

METSPEC 390 is probably the eutectic of the tin-zinc system, although there is some conflict in the published data.
In common with all alloys of low melting point, Metspec 390 undergoes equilibration after solidification. Although melting behavior depends on the age and thermal history of the alloy, the observed differences are of much less significance than those seen in alloys based on bismuth, which melt within a much lower temperature range, where the changes are slower and usually more complex.
The alloy when molten is susceptible to dross formation through oxidation, and a protective atmosphere is recommended. Pressurized nitrogen is preferable to air as the motive gas in spraying.

TENSILE PROPERTIES

Data at 2 Days and 70 Days	BS EN 10 020
Modules of Elasticity	
Proof Stress, 0.2% set	48.5 falling to 42.7 MPa
Tensile Strength	64.3 falling to 54.7 MPa
Elongation (% in 5.65 A)	30 rising to 32.5

HTML Is Not Formatted Properly

HTML Is Not Formatted Properly

HTML Is Not Formatted Properly

HTML Is Not Formatted Properly

TYPICAL USES

METSPEC 390 alloy is used almost exclusively in spraying applications. These are mainly based on the MCP range of spray guns, designed for the rapid formation of alloy moulds for plastics such as polyurethanes. The alloy is suitable for thermal protection devices designed to yield at 197°C.